Mathematical and Computer Modelling 54 (2011) 2616–2622

Contents lists available at SciVerse ScienceDirect

Mathematical and Computer Modelling

journal homepage: www.elsevier.com/locate/mcm

Continuous spectra and numerical eigenvalues

Oksana Guba [a,*], Jens Lorenz [b]

[a] Sandia National Laboratories,[1] PO Box 5800, Albuquerque, NM 87185-1322, United States

[b] Department of Mathematics and Statistics, University of New Mexico, Albuquerque, NM 87131, United States

ARTICLE INFO

Article history:
Received 14 June 2011
Accepted 14 June 2011

Dedicated to Heinz-Otto Kreiss' 80th Birthday

Keywords:
Eigenvalue problems
Continuous spectrum
QR Algorithm

ABSTRACT

Some spectral problems for differential operators are naturally posed on the whole real line, often leading to eigenvalues plus continuous spectrum. Then the numerical approximation typically involves three processes: (a) reduction to a finite interval; (b) discretization; (c) application of a numerical eigenvalue solver such as the QR-algorithm.

Reduction to a finite interval and discretization typically eliminate the continuous spectrum. However, through round-off error, the continuous spectrum may show up again when the eigenvalue solver is applied. (In some sense, three wrongs make a right.) Interestingly, not all parts of the continuous spectrum show up in the same way, however. We illustrate this observation by numerical examples. A perturbation argument, though non-rigorous, explains the observation.

1. On numerical spectra for the linearized Burgers' equation

The stability of a traveling wave depends on the spectrum of a differential operator L obtained by linearization about the wave profile. As a simple example, consider Burgers' equation

$$u_t = u_{xx} - \frac{1}{2}(u^2)_x, \quad x \in \mathbb{R},\ t \geq 0,$$

with stationary solution $U(x) = -\tanh\frac{x}{2}$. Linearization about $U(x)$ leads to the spectral problem

$$Lu \equiv u_{xx} - (Uu)_x = su \quad \text{where } L : H_2(\mathbb{R}) \to L_2(\mathbb{R}). \tag{1}$$

In this case, the operator L has the simple eigenvalue $s_0 = 0$ with corresponding eigenfunction $u_0(x) = U'(x)$. Also, since $U(x) \to \pm 1$ as $x \to \mp\infty$, the operator L has the same continuous spectrum as the operators $L_+u = u_{xx} + u_x$ and $L_-u = u_{xx} - u_x$. Therefore, the continuous spectrum of L is the parabolic line

$$\sigma_{cont} = \{s \in \mathbb{C} \mid s = -k^2 + ik,\ k \in \mathbb{R}\} \tag{2}$$

obtained by applying $L_\pm$ to $u(x) = e^{ikx}$.

Note that L_+ and L_- both have the same continuous spectrum, σ_{cont}, given in (2). Thus, for the operator L in (1) the line (2) should be thought of as double. In the next section we modify Burgers' equation to break the double line into two distinct parabolas. Doing this in two different ways, will more clearly illustrate the main point of the paper.

* Corresponding author.
E-mail addresses: onguba@sandia.gov (O. Guba), lorenz@math.unm.edu (J. Lorenz).

[1] Sandia National Laboratories is a multi-program laboratory operated by Sandia Corporation, a wholly owned subsidiary of Lockheed Martin Corporation, for the US Department of Energy's National Nuclear Security Administration under contract DE-AC04-94AL85000.

0895-7177/$ – see front matter
doi:10.1016/j.mcm.2011.06.037

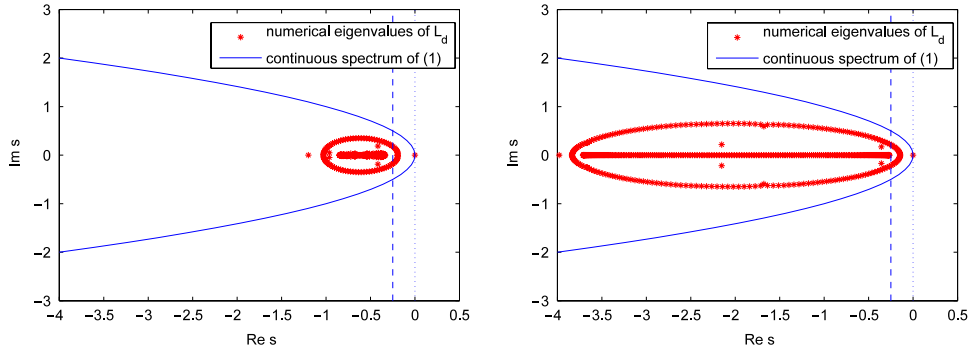

(a) $l = 200$, 220 grid points. (b) $l = 200$, 400 grid points.

Fig. 1. Numerical spectra for stationary Burgers' equation.

To start a numerical approximation, one typically first reduces an all-line problem to a large but finite interval. In case of problem (1), one may impose Dirichlet boundary conditions and consider the eigenvalue problem

$$Lu \equiv u_{xx} - (Uu)_x = su \quad \text{for } -l \le x \le l, \qquad u(-l) = u(l) = 0. \tag{3}$$

Note that (3) is symmetrizable and all eigenvalues are real. Consequently, the continuous spectrum of (1) is not approximated by eigenvalues of (3). (The continuous spectrum of (1) does show up in resolvent estimates for (3), i.e., it is reflected in the pseudospectrum for (3). However, as we will discuss in more detail below, replacing the spectrum by the pseudospectrum is not the main point of this paper.)

Discretization of (3) on a uniform grid with 2nd-order centered differences leads to the matrix eigenvalue problem $L_d u = su$ where

$$L_d = \begin{pmatrix} -\frac{2}{h^2} & \frac{1}{h^2} - \frac{U_3}{2h} & 0 & \cdots & 0 \\ \frac{1}{h^2} + \frac{U_2}{2h} & -\frac{2}{h^2} & \frac{1}{h^2} - \frac{U_4}{2h} & \cdots & 0 \\ & \ddots & \ddots & \ddots & \\ 0 & \cdots & \frac{1}{h^2} + \frac{U_{n-3}}{2h} & -\frac{2}{h^2} & \frac{1}{h^2} - \frac{U_{n-1}}{2h} \\ 0 & \cdots & 0 & \frac{1}{h^2} + \frac{U_{n-2}}{2h} & -\frac{2}{h^2} \end{pmatrix}. \tag{4}$$

Here $h = 2l/(n-1)$, $x_i = -l + (i-1)h$, $U_i = U(x_i) = -\tanh(x_i/2)$ and L_d has dimension $(n-2) \times (n-2)$. If $h < 2$ then L_d is symmetrizable and all eigenvalues of L_d are real. However, using the MATLAB command

```
>eig(Ld,'nobalance');
```

one obtains numerical eigenvalues which are not real. See Fig. 1 for the results.

We refer to the computed approximations of matrix eigenvalues as *numerical eigenvalues*. Because of the continuous spectrum (2), the occurrence of complex numerical eigenvalues of L_d is not unexpected.

In Section 3 we simplify the variable-coefficient problem (3) and consider the two constant-coefficient problems

$$L_{\pm}u \equiv u_{xx} \pm u_x = su \quad \text{for } -l \le x \le l, \qquad u(-l) = u(l) = 0. \tag{5}$$

Discretization leads to two matrix eigenvalue problems

$$L_{d+}u = su \quad \text{and} \quad L_{d-}u = su \tag{6}$$

with matrices L_{d+} and L_{d-} which have the same eigenvalues and the same pseudospectra since L_{d-} is the transpose of L_{d+}. Nevertheless, the numerical eigenvalues of L_{d+} and L_{d-} turn out to be quite different from each other: For certain values of the step size h, the numerical eigenvalues of L_{d-} become complex whereas those of L_{d+} remain real. This observation, which will be explained by a perturbation argument, is the main point of the paper.

There is, of course, a large amount of literature on some of the issues addressed in this paper. We comment on the literature in the last section.

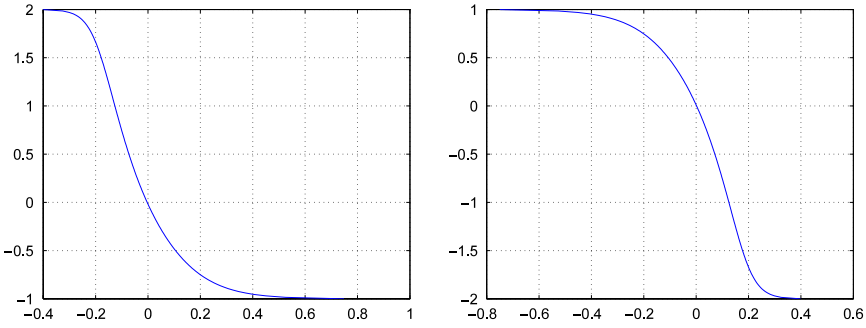

(a) Profile $U(x)$. (b) Profile $V(x)$.

Fig. 2. Profiles $U(x)$ and $V(x)$ for Problems 1 and 2.

2. Two scalar conservation laws

For the linearized Burgers' equation, the continuous spectra of $L_+ = u_{xx} + u_x$ and $L_- = u_{xx} - u_x$ are identical. In the following two problems, this symmetry is broken.

Problem 1.

$$u_t = u_{xx} - f(u)_x \quad \text{with } f(u) = u^4 - 5u \tag{7}$$

and

Problem 2.

$$u_t = u_{xx} - g(u)_x \quad \text{with } g(u) = u^4 + 5u. \tag{8}$$

First consider Problem 1. Since $f(2) = f(-1) = 6$ and $f(u) < f(6)$ for $-1 < u < 2$, Eq. (7) has a stationary solution $U(x)$ with[2]

$$U(-\infty) = 2, \qquad U(\infty) = -1. \tag{9}$$

The profile $U(x)$ is shown in Fig. 2(a).

The continuous spectrum of the linearized operator

$$Lu = u_{xx} - (f'(U(x))u)_x \tag{10}$$

is the union of the continuous spectra of

$$L_+u = u_{xx} - f'(U(\infty))u_x$$

and of

$$L_-u = u_{xx} - f'(U(-\infty))u_x.$$

Since $f'(-1) = -9$ and $f'(2) = 27$ one obtains the two parabolas

$$s = -k^2 + 9ik \quad \text{and} \quad s = -k^2 - 27ik, \quad k \in \mathbb{R}, \tag{11}$$

as the continuous spectrum of the operator L given in (10).

Now consider Problem 2 specified in Eq. (8). Since $g(-2) = g(1) = 6$ and $g(u) < g(6)$ for $-2 < u < 1$, Eq. (8) has a stationary solution $V(x)$ with

$$V(-\infty) = 1, \quad V(\infty) = -2. \tag{12}$$

The profile $V(x)$ is shown in Fig. 2(b).

The continuous spectrum of the linearized operator

$$Mu = u_{xx} - (g'(V(x))u)_x \tag{13}$$

is the union of the continuous spectra of

$$M_+u = u_{xx} - g'(V(\infty))u_x$$

[2] The profile $U(x)$ can be obtained by solving $U_x = f(U) - f(6)$, $U(0) = 0$. Without the normalization $U(0) = 0$, the profile can be shifted arbitrarily.

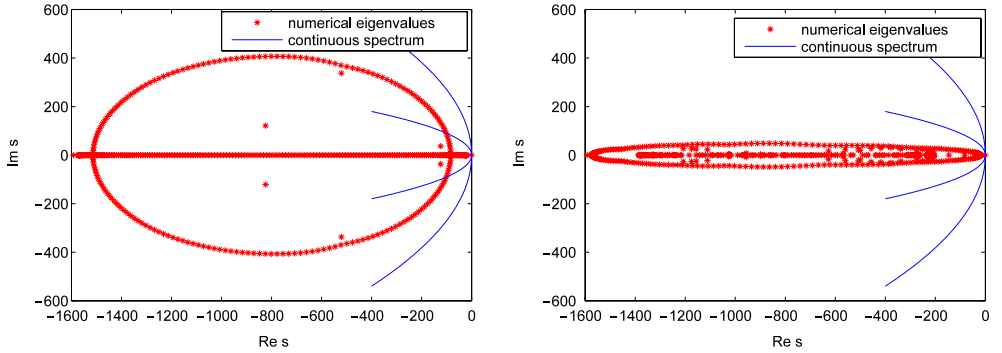

(a) $f(u) = u^4 - 5u$, $l = 10$, $n = 400$. (b) $g(u) = u^4 + 5u$, $l = 10$, $n = 400$.

Fig. 3. Approaching wide and narrow parabolas.

and of

$$M_- u = u_{xx} - g'(V(-\infty))u_x.$$

Since $g'(1) = 9$ and $g'(-2) = -27$ one obtains the two parabolas

$$s = -k^2 - 9ik \quad \text{and} \quad s = -k^2 + 27ik, \quad k \in \mathbb{R}, \tag{14}$$

as the continuous spectrum of the operator M given in (13).

It is then obvious that the two operators L and M have the same continuous spectrum. It consists of two parabolas, a wider one, $s = -k^2 + 27ik$, and a narrower one, $s = -k^2 + 9ik$. Here $k \in \mathbb{R}$ is a parameter. One might expect that the numerical process outlined above (consisting of cut-off, discretization, and application of QR) will lead to almost identical approximations. This is not the case, however.

Fig. 3(a) shows the numerical spectrum of the matrix L_d, obtained similarly as (4), from the operator (10). Here we use the difference formula

$$(f'(U)u)_x(x_i) \sim \frac{1}{2h}\left(f'(U(x_{i+1}))u_{i+1} - f'(U(x_{i-1}))u_{i-1}\right).$$

Since $|f'(U(x))| \leq 27$ the matrix L_d is diagonalizable with real eigenvalues as long as

$$\frac{1}{h^2} - \frac{27}{2h} > 0.$$

This condition is satisfied for the computations shown in Fig. 3(a). However, the numerical spectrum shows a large number of complex eigenvalues, forming the elliptic curve in the figure.

If one proceed similarly for the operator M in (13), one obtains the results shown in Fig. 3(b). Now the complex numerical eigenvalues lie on a narrow elliptic curve.

Recall that the operators L and M both have the same continuous spectrum, consisting of two parabolas. The two parabolas are also indicated in Fig. 3. We now try to give a reason for the observed difference in the numerical spectra for L and M and refer to the next section for further details. For the operator L the continuous spectrum comes from

$$u_{xx} - 27u_x = su \tag{15}$$

and

$$u_{xx} + 9u_x = su. \tag{16}$$

In contrast, for the operator M the continuous spectrum comes from

$$u_{xx} + 27u_x = su \tag{17}$$

and

$$u_{xx} - 9u_x = su. \tag{18}$$

After cut-off, discretization, and application of QR, the continuous spectrum of (15) (wide parabola) and the continuous spectrum of (18) (narrow parabola) show up. Note that in both equations, (15) and (18), the coefficient of the u_x-term is negative. In contrast, the continuous spectra of (16) and (17), where the coefficient of the u_x-term is positive, are not reflected in the numerical spectra. Simplifying, we discretize the two eigenvalue problems $u_{xx} + u_x = su$ and $u_{xx} - u_x = su$ in the next section. Discretizations of $u_{xx} + u_x$ lead to a matrix with entries

$$\frac{1}{h^2} - \frac{1}{2h}, \qquad -\frac{2}{h^2}, \qquad \frac{1}{h^2} + \frac{1}{2h}$$

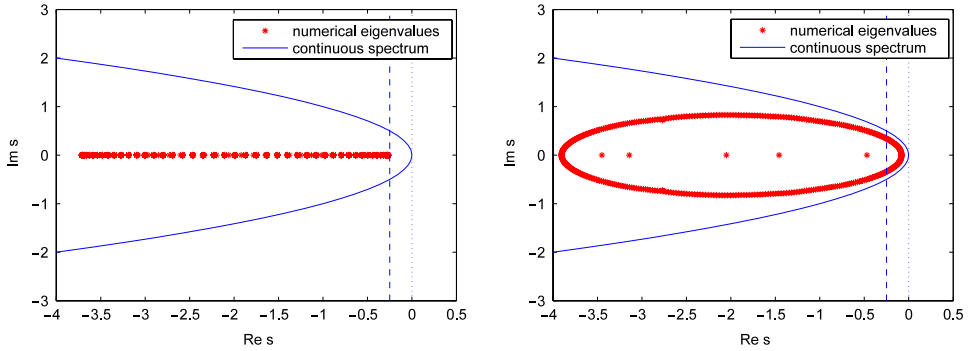

(a) $L_+u = u'' + u'$, $l = 200$, 400 grid points. (b) $L_-u = u'' - u'$, $l = 200$, 400 grid points.

Fig. 4. Numerical spectra for $L_\pm u = u'' \pm u'$.

near the diagonal. The larger outer diagonal entry $\frac{1}{h^2} + \frac{1}{2h}$ occurs *above* the main diagonal. The spectrum of the resulting matrix L_d is then sensitive to perturbations *below* the main diagonal. In contrast, discretization of $u_{xx} - u_x$ leads a matrix with entries

$$\frac{1}{h^2} + \frac{1}{2h}, \qquad -\frac{2}{h^2}, \qquad \frac{1}{h^2} - \frac{1}{2h}$$

near the diagonal and the larger outer diagonal entry $\frac{1}{h^2} + \frac{1}{2h}$ occurs *below* the main diagonal. This makes the spectrum of L_d sensitive to perturbations *above* the main diagonal. Since the *QR*-algorithm produces round-off errors *above* the main diagonal, the spectrum in the second case gets perturbed considerably, leading to complex numerical eigenvalues. In the first case, the spectrum of L_d is insensitive to the perturbations above the main diagonal, and the *QR*-algorithm produces accurate real eigenvalues. The same phenomena prevail for the numerical spectra corresponding to the operators L and M.

3. Further numerical results and explanation

Applying 2nd-order centered differences to (5) one obtains the matrix eigenvalue problems (6). In Fig. 4 we show the numerical eigenvalues of L_{d+} and L_{d-} for $l = 200$ and 400 grid points. The graphs also show the continuous spectrum (2). The exact eigenvalues of L_{d+} and L_{d-} obviously agree since $(L_{d+})^T = L_{d-}$, but the *QR*-algorithm affects the two matrices differently, leading to different numerical eigenvalues.

To focus on the essential issue, we simplify further and consider Toeplitz matrices of the form

$$A = \begin{pmatrix} 0 & 1 & 0 & 0 & \dots & \\ a & 0 & 1 & 0 & \dots & \\ 0 & a & 0 & 1 & \dots & \\ & & \ddots & \ddots & \ddots & \\ & \dots & 0 & a & 0 & 1 \\ & \dots & 0 & 0 & a & 0 \end{pmatrix} \in \mathbb{R}^{n\times n}, \tag{19}$$

where $a \gg 1$. We will also consider the transpose, A^T.

Using the LAPACK routine DLAHQR, we obtain numerical eigenvalues for A and A^T as shown in Fig. 5. The figure also shows the exact eigenvalues. Clearly, the numerical eigenvalues of A^T are reasonably close to the exact eigenvalues, but those of A are affected strongly by the numerical process.

We now show that the eigenvalues of the two matrices, A and A^T, are sensitive to perturbations in a different way, which explains why the *QR*-algorithm produces significantly different results. Consider the matrix $E = (e_{ij}) \in \mathbb{R}^{n\times n}$ with entries $e_{ij} = 0$ except for $e_{1n} = 1$. Let $T_n(\lambda, \varepsilon) = \det(A + \varepsilon E - \lambda I)$ denote the characteristic polynomial of the perturbed matrix $A + \varepsilon E$. Correspondingly, let $\widetilde{T}_n(\lambda, \varepsilon) = \det(A^T + \varepsilon E - \lambda I)$. We then have

$$\begin{aligned} T_n(\lambda, \varepsilon) &= -\lambda T_{n-1}(\lambda, 0) - aT_{n-2}(\lambda, 0) - (-1)^n \varepsilon a^{n-1} \\ \widetilde{T}_n(\lambda, \varepsilon) &= -\lambda T_{n-1}(\lambda, 0) - aT_{n-2}(\lambda, 0) - (-1)^n \varepsilon. \end{aligned}$$

Clearly, the perturbation term εa^{n-1} in $T_n(\lambda, \varepsilon)$ is larger by a factor a^{n-1} than the perturbation term in $\widetilde{T}_n(\lambda\varepsilon)$. (For the example illustrated in Fig. 5, this factor is 10^{38}.)

More generally, the spectrum of A is much more sensitive to perturbations above the main diagonal than to perturbations below. We illustrate this in Fig. 6. The opposite holds true for A^T. Since the *QR*-algorithm introduces perturbations *above* the main diagonal, the numerical eigenvalues of A^T agree well with the exact eigenvalues, but this is not the case for the matrix A. The same arguments can be applied to the matrices $L_{d\pm}$ given above if $0 < \frac{1}{h^2} - \frac{1}{2h} \ll \frac{1}{h^2} + \frac{1}{2h}$.

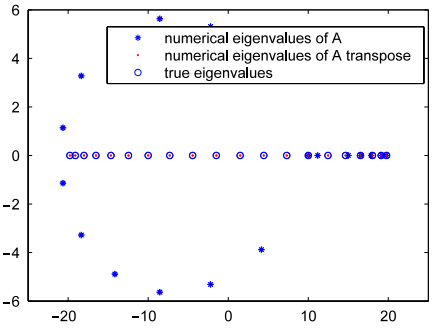

Fig. 5. Numerical spectra of A and A^T, $n = 20$, $a = 100$, obtained by routine DLAHQR.

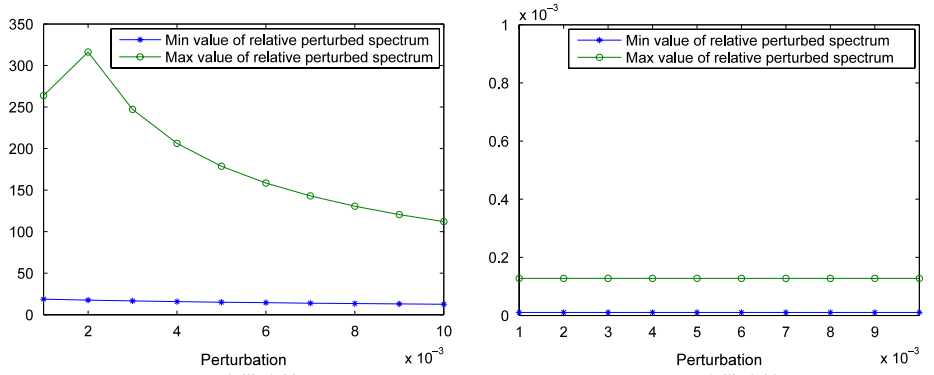

(a) Min and max values of $|\frac{\lambda_i(0)-\lambda_i(\varepsilon)}{\varepsilon}|$, $\lambda_i \in \sigma(A+\varepsilon E)$, $i = 1, \ldots, n$.

(b) Min and max values of $|\frac{\lambda_i(0)-\lambda_i(\varepsilon)}{\varepsilon}|$, $\lambda_i \in \sigma(A+\varepsilon E^T)$, $i = 1, \ldots, n$.

Fig. 6. Relative perturbations of spectrum for A.

3.1. Remarks on Fig. 6

For the results of Fig. 6 we considered the matrix A given in (19) with $n = 10$ and $a = 5$. Also, we recall that $E = (e_{ij})$ where $e_{ij} = 0$ except for $e_{15} = 1$. If $\lambda_i(\varepsilon)$ denotes the eigenvalues of $A + \varepsilon E$, then the upper curve in Fig. 6 (a) shows the relative error

$$\max_{1\le i\le 10} \frac{1}{\varepsilon}|\lambda_i(0) - \lambda_i(\varepsilon)|$$

where $10^{-3} \le \varepsilon \le 10^{-2}$. Here the perturbation εE is introduced above the main diagonal. If εE^T is added to A, the relative error becomes much smaller as shown in Fig. 6, (b).

3.2. Remarks on the perturbation argument

Instead of considering the characteristic polynomial of $A + \varepsilon E$ (with A given in (19)), one can also argue as follows: If $b = \sqrt{a}$ and $D = \mathrm{diag}(b, b^2, \ldots, b^n)$, then $D^{-1}AD = A_{sym}$ is symmetric and

$$D^{-1}(A + \varepsilon E)D = A_{sym} + \varepsilon b^{n-1}E$$
$$D^{-1}(A + \varepsilon E^T)D = A_{sym} + \frac{\varepsilon}{b^{n-1}}E^T.$$

Taking, for example, $n = 20$, $a = 100$ as above, we see that the perturbation $\varepsilon b^{n-1}E$ of the symmetrized matrix A_{sym} exceeds the perturbation $\frac{\varepsilon}{b^{n-1}}E^T$ in size by a factor 10^{38}.

4. Summary and comments on the literature

We started with the all-line spectral problem (1) and its continuous spectrum (2). A numerical process to approximate the spectrum, typically involves three parts: reduction to a finite interval; discretization; an eigenvalue solver. It is interesting to note that the numerical error of the eigenvalue solver may, or may not, compensate for the error of reduction (which, in

the cases considered here, leads to a real spectrum) and reintroduce a complex-valued numerical spectrum. Due to different sensitivities of the spectra of a matrix and of its its transpose, the QR-algorithm treats matrices A and A^T differently.

For results relating spectra of all-line problems and finite-interval problems see, for example, [1–5]. For the distinction between stability on a finite interval in contrast to the whole line see, for example, [6].

The importance of the pseudospectrum and its influence on numerical eigenvalues is addressed in [7]. Extensive studies of the pseudospectra of Toeplitz matrices and their modifications are given in [8–11]. The paper [8] also notices that numerical algorithms can lead to different results when applied to A and A^T and suggestions are made for diagonal scalings to obtain an eigenvalue problem that is better conditioned.

Acknowledgments

The authors would like to thank David Day, Sandia National Laboratories, for sharing his insight into sensitivities of eigenvalues of A and A^T.

References

[1] B. Sandstede, A. Scheel, Absolute and convective instabilities of waves on unbounded and large bounded domains, Physica D 145 (3–4) (2000) 233–277.
[2] W.-J. Beyn, J. Lorenz, Stability of traveling waves: dichotomies and eigenvalue conditions on finite intervals, Numer. Funct. Anal. Optim. 20 (3–4) (1999) 201–244.
[3] O. Guba, The Spectra of Differential Operators: Bounded and Unbounded Domains, VDM Verlag, Saarbrücken, 2009.
[4] O. Guba, Convergence of Green's functions of ordinary differential equations, Math. Comput. Modelling 50 (3–4) (2009) 542–555. doi:10.1016/j.mcm.2009.03.008.
[5] O. Guba, Using root functions for eigenvalue problems of ordinary differential operators, Numer. Funct. Anal. Optim. 30 (11–12) (2009) 1289–1308. doi:10.1080/01630560903439197.
[6] G. Kreiss, H.-O. Kreiss, J. Lorenz, Stability of viscous shocks on finite intervals, Arch. Ration. Mech. Anal. 187 (1) (2008) 157–183. doi:10.1007/s00205-007-0073-5.
[7] S.C. Reddy, L.N. Trefethen, Pseudospectra of the convection-diffusion operator, SIAM J. Appl. Math. 54 (6) (1994) 1634–1649.
[8] R.M. Beam, R.F. Warming, The asymptotic spectra of banded Toeplitz and quasi-Toeplitz matrices, SIAM J. Sci. Comput. 14 (4) (1993) 971–1006. doi:10.1137/0914059.
[9] A. Böttcher, S.M. Grudsky, Spectral Properties of Banded Toeplitz Matrices, Society for Industrial and Applied Mathematics (SIAM), Philadelphia, PA, 2005.
[10] L.N. Trefethen, M. Embree, Spectra and Pseudospectra, Princeton University Press, Princeton, NJ, 2005, the behavior of nonnormal matrices and operators.
[11] L. Reichel, L.N. Trefethen, Eigenvalues and pseudo-eigenvalues of Toeplitz matrices, Linear Algebra Appl. 162/164 (1992) 153–185. doi:10.1016/0024-3795(92)90374-J. directions in matrix theory (Auburn, AL, 1990).